Canadian Chemical Transactions Year 2015 | Volume 3 | Issue 2 | Page 158-170

*Research Article*

DOI:10.13179/canchemtrans.2015.03.02.0175

# Photophysical, Electrochemical and Thermal Studies of 5-methyl-5*H*-Benz[*g*]indolo[2,3-*b*]quinoxaline Derivatives: Green and Yellow Fluorescent Materials

**Azam M. Shaikh, Bharat K. Sharma and Rajesh M. Kamble***

*Department Of Chemistry, University Of Mumbai, Santacruz (East), Mumbai–400 098 (India)*

*Corresponding Author: Email: kamblerm@chem.mu.ac.in*

***Received:*** *February 20, 2015* ***Revised:*** *April 7, 2015* ***Accepted:*** *April 11, 2015* ***Published:*** *April 13, 2015*

**Abstract:** In this work, 5-methyl-5*H*-Benz[*g*]indolo[2,3-*b*]quinoxaline ($BIQCH_3$) and its derivatives were prepared in good yield by condensing 5-Substituted-1-methyl-1*H*-Indole-2,3-dione and 2,3-diaminonaphthalene in glacial acetic acid. The structure of $BIQCH_3$ and its derivatives were confirmed using FT−IR, $^1$H NMR, $^{13}$C NMR, Mass spectra and elemental analysis. The photophysical and electrochemical studies of $BIQCH_3$ and its derivatives were studied by UV-Visible spectroscopy, fluorescence spectroscopy and cyclic voltammetry respectively. The optical energy band gap of $BIQCH_3$ and its derivatives lies in the range of 2.53−2.58 eV. Thermal analysis of $BIQCH_3$ and its derivative were studied by Thermo Gravimetric Analysis (TGA) and Differential Thermal Analysis (DTA).

**Keywords:** Green–yellow Electroluminescent Material, Photophysical Properties, Electrochemical Properties, Thermal Properties.

## 1. INTRODUCTION

In last few decades there is a significant progress in the field of Organic electronics which includes Organic light emitting diodes (OLEDs) [1–3], Organic field effect transistors (OFETs) [4] and Dye sensitized solar cells (DSSCs) [5–7]. Molecules containing Donor-acceptor (D–A) core have been found to exhibit interesting charge-transporting characteristics in electroluminescent devices [8]. Indolo[2,3-*b*]quinoxaline and their derivatives are very important class of nitrogen containing heterocyclic compounds and have been widely used in dyes [9], photoinitiator [10] and Optical devices [11–14]. Indolo[2,3-*b*]quinoxalines not only possess many important applications in material sciences, but also in medicinal chemistry. Earlier research showed that indolo[2,3-*b*]quinoxaline derivatives exhibit a wide range of interesting biological activities, such as antiviral [15,16] anticancer [17,18] antimicrobial [19] and antibacterial activities [20].

Benz[*g*]indolo[2,3-*b*]quinoxalines is a built in donor–acceptor chromophores as it contain the electron rich indole unit fused with electron deficient quinoxaline moiety, however they are reported in literature [21,22] and are used in medicinal chemistry as an antiviral and anticancer agents [23,24]. Considering the importance of indolo[2,3-*b*]quinoxalines in material sciences it was decided to investigate the optoelectronic and thermal properties of Benz[*g*]indolo[2,3-*b*]quinoxalines. To the best of our knowledge the optoelectronic and thermal properties of Benz[*g*]indolo[2,3-*b*]quinoxalines have not

been yet explored. The optoelectronic properties of Benz[*g*]indolo[2,3-*b*]quinoxalines can be readily tuned by introducing electron donating or electron withdrawing group at second position of indole unit of Benz[*g*]indolo[2,3-*b*]quinoxalines.

In this paper we report the photophysical, electrochemical and thermal properties of 5-methyl-5*H*-Benz[*g*]indolo[2,3-*b*]quinoxaline ($BIQCH_3$) and its derivatives (**Chart 1**) by substituting second position of $BIQCH_3$ (**1**) with electron donating and electron withdrawing groups such as $–CH_3$ and –Br, $–NO_2$ respectively. The studies also explores the effects of electron donating and electron withdrawing group at second position of $BIQCH_3$ on electrochemical properties such as HOMO and LUMO energy levels and photophysical properties.

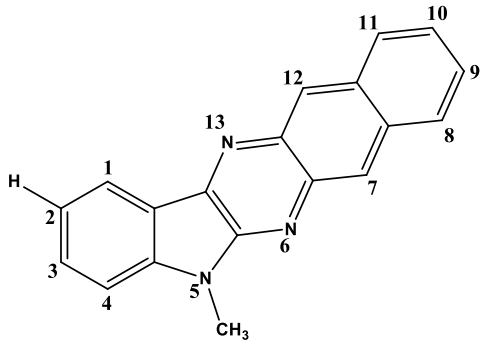


**$BIQCH_3$ (1)**

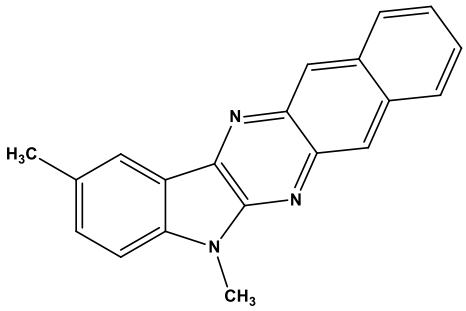


**$BIQCH_3CH_3$ (2)**

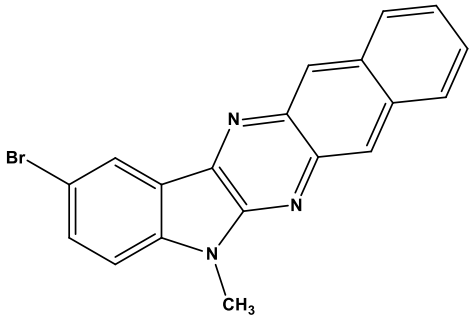


**$BIQCH_3Br$ (3)**

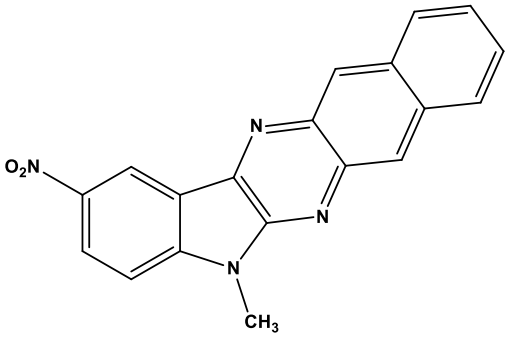


**$BIQCH_3NO_2$ (4)**

**Chart 1:** Molecular structures of $BIQCH_3$ and its derivatives **1**–**4**.

## 2. EXPERIMENTAL SECTION

### *2.1 Materials and Equipments*

All the starting materials and reagents were purchased from commercial source (S D fine and Alfa Aesar) and were used without any further treatment and purifications unless otherwise noted. The organic solvents were of HPLC and spectroscopic grade and were dried and freshly distilled using the standard procedures and handled in moisture free atmosphere.

Investigation and confirmation of chemical structures of all the prepared molecules were done using FT-IR, $^1$H NMR, $^{13}$C NMR, MASS spectra and Elemental analysis. $^1$H NMR spectra and $^{13}$C NMR spectra were recorded using $CDCl_3$ on a Bruker 300 Ultrashield spectrometer with Tetramethylsilane

(TMS) as internal reference at a working frequency of 300 MHz and 75 MHz respectively. Fourier transform infrared (FT-IR) spectra were recorded on a Perkin Elmer Frontier 91579. Elemental analysis was recorded on Euro EA elemental analyzer and Mass spectra were recorded on Thermo scientific GC-MS. HRMS spectra of $BIQCH_3NO_2$ (**4**) was recorded on maxis impact 282001.00081 instrument.

UV−Visible spectra were recorded for $10^{-5}$ M toluene solutions in a 1 cm path length quartz cuvette as well as thermally deposited thin solid films, on SHIMADZU U.V–2401PC at room temperature. The excitation and emission spectra were carried out on a Perkin Elmer LS 55 Fluorescence spectrophotometer. Optical band gap energy was taken from the intersection of normalized excitation and emission spectra. The fluorescence quantum yields ($\phi_F$) were calculated relative to tris(8-hydroxyquinolinato)aluminium(III) ($Alq_3$) in benzene ($\phi_F$ =0.16) [25] as a standard for green emitting materials.

Cyclic voltammetry studies was carried out on a computer controlled AUTOLAB PGSTATE 30 electrochemical analyzer equipped with USB electro chemical interface using GPES software version 4.9.005. Typically, a three electrode cell equipped with a glassy carbon working electrode, Ag/AgCl (non-aqueous) reference electrode and platinum (Pt) wire as counter electrode was employed. The measurements have been carried at room temperature in anhydrous dichloromethane ($10^{-3}$ M) with $Bu_4NPF_6$ (0.1 M) as supporting electrolyte with a scan rate of 100 $mVs^{-1}$. The potential of Ag/AgCl reference electrode was calibrated by using ferrocene/ferrocenium redox couple which has the known oxidation potential of + 4.8 eV.

The Ionization potential (HOMO) is calculated from peak potentials ($E_{oxi}$) of the oxidation event according to the equation (1). Electron affinity (LUMO) energy values are calculated from peak potentials ($E_{red}$) of the reduction event according to the equation (2).

$$E_{HOMO} = -\left[ E_{oxi}^{peak} - E_{oxi}\left( Fc/Fc^{+}\right) + 4.8 \right] eV \quad (1)$$

$$E_{LUMO} = -\left[ E_{red}^{peak} - E_{red}\left( Fc/Fc^{+}\right) + 4.8 \right] eV \quad (2)$$

Melting points of the products were determined by open capillary method and compared with Differential Thermal analysis (DTA). The thermo gravimetric analysis (TGA) was performed using Perkin Elmer Pyris Diamond TG/DTA under nitrogen atmosphere. Column chromatography was carried out using SD−Fine silica gel (60−120 mesh), eluting with n−hexane and chloroform. The progress of reaction and the purity of the compound were checked by thin layer chromatography (TLC) on silica gel coated glass plates, in which the spots were visualized with UV light and in iodine chamber.

### *2.2 Synthesis and Characterization*

5-Substituted-1-methyl-1*H*-Indole-2,3-dione is prepared according to the reported procedure [26−28]. Compound **1–4** was prepared by condensation of 5-Substituted-1-methyl-1*H*-Indole-2,3-dione and 2,3-diaminonaphthalene in acetic acid. Preparation of $BIQCH_3$ (**1**), $BIQCH_3Br$ (**3**) and $BIQCH_3NO_2$ (**4**) are reported in literature [21,22]. However $BIQCH_3CH_3$ (**2**) is not reported and all of these compounds are confirmed by FT-IR, $^1$H NMR, $^{13}$C NMR, MASS spectra and elemental analysis. Due to the poor solubility of $BIQCH_3NO_2$ (**4**) in various solvent we could not get the $^1$H NMR, $^{13}$C NMR spectra but it is confirmed by Mass spectra and High Resolution Mass Spectra (HRMS). The detailed synthetic route adopted for the synthesis of $BIQCH_3$ and its derivatives **1–4** is depicted in **Scheme 1** and molecular structures of the prepared derivatives are illustrated in **Chart 1**.

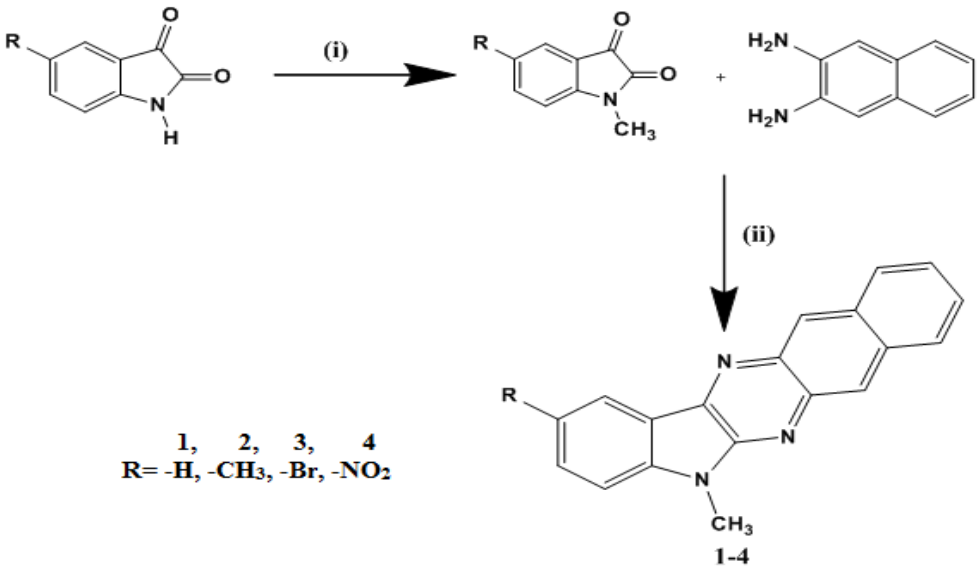


**Reaction condition:** (i) anhydrous $K_2CO_3/CH_3I$, DMF, Reflux, 15 hrs.

(ii) $CH_3COOH$, Reflux, 3hrs.

**Scheme 1**: Preparation of $BIQCH_3$ and its derivatives **1–4**.

*2.2.1 General procedure for the preparation of $BIQCH_3$ and its derivatives **1–4**:*

A mixture of 5-Substituted-1-methyl-1*H*-Indole-2,3-dione (1 mmol) and 2,3-diamino naphthalene (108 mg, 1 mmol) was dissolved in glacial acetic acid (10 ml). The reaction mixture was continuously stirred at 100 $^0$C for 3 hrs. After completion of reaction, reaction mixture is poured in cold distilled water and filtered, and washed with water. The solid thus obtained was then purified by column chromatography (eluent: n-hexane: chloroform ratio as 70:30) to obtain a yellow to orange solid.

*2.2.1.1. Preparation of 5-methyl-5H-Benz[g]indolo[2,3-b]quinoxaline ($BIQCH_3$) (**1**)*

Yield: 212 mg (75.0 %), M.P.: 238 $^o$C. MS: $C_{19}H_{13}N_3$, *m/z*: 284.17 $[M+1]^+$. Anal.Calcd for $C_{19}H_{13}N_3$: C (80.54), H (4.62), N (14.84). Found: C (80.56), H (4.62), N (14.82). IR (neat, $\nu_{max}$ $cm^{-1}$): 1112, 1274, 1496, 2922, 3049; $^1$H NMR ($CDCl_3$, 300 MHz): δ (ppm) 3.84 (s, 3H,−$CH_3$), 7.35 (q, 2H, ArH, *J* =7.5 Hz, 9 Hz), 7.45 (q, 2H, ArH *J* = 6.6 Hz, 7.2 Hz), 7.63 (t, 1H, ArH, *J* = 8.1 Hz), 8.40 (d, 2H, ArH, *J* =7.5 Hz ), 8.08 (dd, 2H, ArH, J = 8.1 Hz), 8.80 (s, 1H, ArH); $^{13}$C NMR ($CDCl_3$, 75 MHz): δ (ppm) 27.35, 109.00, 119.00, 121.07,122.97, 124.49, 125.01, 126.16, 127.58, 127.68, 128.36, 131.31, 131.81, 133.34, 137.16, 137.71, 142.73, 146.14, 146.37.

*2.2.1.2. Preparation of 2, 5-dimethyl-5H-Benz[g]indolo[2,3-b]quinoxaline ($BIQCH_3CH_3$) (**2**)*

Yield: 208 mg (70.0 %), M.P.: 215 $^o$C. MS: $C_{20}H_{15}N_3$, *m/z*: 298.36 $[M+1]^+$. Anal.Calcd for $C_{19}H_{13}N_3$: C (80.78), H (5.09), N (14.13). Found: C (80.77), H (5.08), N (14.15).IR (neat, $\nu_{max}$ $cm^{-1}$): 1113,1391, 1578, 1605, 2852, 2919, 3044; $^1$H NMR ($CDCl_3$, 300 MHz): δ (ppm) 2.49 (s, 3H,−$CH_3$), 3.84 (s, 3H,−$CH_3$), 7.37−7.52 (m, 4H, ArH), 8.04 (dd, 2H, ArH, *J* = 7.8 Hz, 8.1 Hz), 8.15 (s, 1H, ArH), 8.49 (s, 1H, ArH), 8.73 (s, 1H, ArH); $^{13}$C NMR ($CDCl_3$, 75 MHz): δ (ppm) 21.12, 27.31, 108.64, 119.37, 122.98, 124.34,

124.88, 126.04, 127.48, 127.65, 128.33, 130.58, 131.18, 132.76, 133.24, 137.06, 137.68, 142.70, 144.21, 146.45.

*2.2.1.3. Preparation of 2-bromo-5-methyl-5H-Benz[g]indolo[2,3-b]quinoxaline (BIQCH$_3$Br) (**3**)Yield:* 260 mg (72.0 %), M.P.: 274 $^{o}$C. MS: $C_{19}H_{12}BrN_3$, *m/z*: 362.53 $[M]^+$. Anal.Calcd for $C_{19}H_{13}BrN_3$: C (63.00), H (3.34), N (11.60), Br (22.06). Found: C (63.03), H (3.31), N (11.61), Br (22.05). IR (neat, $\nu_{max}$ cm$^{-1}$): 1271, 1449, 1580, 1598, 2920, 3045; $^1$H NMR ($CDCl_3$, 300 MHz): δ (ppm) 3.90 (s, 3H,−$CH_3$), 7.27-7.59 (m, 2H, ArH), 7.78 (dd, 2H, ArH *J* = 2.1 Hz, 6.6 Hz), 8.12 (dd, 2H, ArH, *J* = 1.5 Hz, 5.7 Hz ), 8.56 (s, 1H, ArH), 8.62 (s, 1H, ArH), 8.83 (s, 1H, ArH) ; $^{13}$C NMR ($CDCl_3$, 75 MHz): δ (ppm) 27.62, 110.57, 124.70, 125.35, 125.81, 126.55, 127.76, 127.90, 128.30, 128.47, 128.56, 129.03, 129.23, 130.08, 131.48, 131.57, 132.50, 134.36, 144.78.

*2.2.1.4. Preparation of 2-nitro-5-methyl-5H-Benz[g]indolo[2,3-b]quinoxaline (BIQCH$_3$NO$_2$) (**4**)*

Yield: 132 mg (40.0 %), M.P.: >300 $^{o}$C. MS: $C_{19}H_{12}N_4O_2$ *m/z*: 327.83 $[M]^+$. HRMS cal for $C_{19}H_{13}N_4O_2$ 329.1033, found 329.1035. Anal.Calcd for $C_{19}H_{12}N_4O_2$: C (69.51), H (3.68), N (17.06) O (9.75). Found: C (69.55), H (3.69), N (17.02) O (9.74). IR (neat, $\nu_{max}$ cm$^{-1}$): 1271, 1292, 1332, 1591, 1592, 2849, 2918, 3087.

## 3. RESULTS AND DISCUSSIONS

### 3.1 Photophysical properties

The photophysical properties of compound BIQCH$_3$ and its derivatives **1–4** are depend on entire Benz[*g*]indolo[2,3-*b*]quinoxaline core and substituents on its second position. The photophysical studies were performed on the $10^{-5}$ M solution of BIQCH$_3$ and its derivatives **1–4** in toluene and thin solid film respectively using UV–Vis absorption and fluorescence spectroscopy. Thin films of BIQCH$_3$ and its derivatives **1–4** was prepared by spin coating method using $10^{-3}$ M solution of BIQCH$_3$ and its derivatives **1–4** in toluene on silica quartz plates. Basic photophysical characteristics such as the absorption maxima ($\lambda_{Abs}$), fluorescence maxima ($\lambda_{Em}$), molar extinction coefficient (ε), optical band gaps ($E_g^{opt}$), Stokes shift ($\nu_{Abs} - \nu_{Em}$) and fluorescent quantum yield ($\phi_F$) of the molecules were determined and pertinent data is summarized in **Table 1** and the spectral profiles are displayed in **Figure 1** and **2**.

The absorption spectra of BIQCH$_3$ and its derivatives **1–4** are dominated by the intense overlapping bands with $\lambda_{Abs}$ below 300 nm are due n–$\pi^*$ transition originating from electron donating indole unit and 311–396 nm mainly due to $\pi-\pi^*$ transition arising from entire Benz[*g*]indolo[2,3-*b*]quinoxaline core. Further, a lower intensity absorption broad band above 400 nm observed which may be due to charge transfer between the electron–donating indole and the electron–accepting benzo[*g*]quinoxaline core. In BIQCH$_3$NO$_2$ (**4**) intensity of $\pi-\pi^*$ transition and charge transfer transition is slightly high as compared to other derivatives suggesting better charge transfer due to electron withdrawing $NO_2$ group.

The absorption spectra for all the compounds in thin films are found to be slightly broader in nature as compared to solution form and this may be due to intermolecular aggregation of the molecules in the solid state. However peaks are distinct and of nearly same order relative to solution form.

Optical band gap ($E_g^{opt}$) for the derivatives are calculated from the solution state absorption and excitation spectra and are in the range 2.53–2.58 eV (**Table 1**). Molar extinction coefficients (ε) of the derivatives are recorded at λmax value obtained from absorption spectra and are high in the range 17741–27797 which indicates that the long wavelength band of the absorption spectrum is a charge transfer band through the π–π* transition.

**Table 1:** Photophysical data of $BIQCH_3$ and its derivatives **1–4**

| Compound | $\lambda_{abs}$ (nm)[a] | | $\lambda_{emi}$ (nm)[a] | | ε[b] | $E_g^{opt}$ (eV)[c] | Stoke shift[d] ($cm^{-1}$) | $\phi_F$[e] |
|---|---|---|---|---|---|---|---|---|
| | sol | film | sol | film | | | | |
| $BIQCH_3$ | 296,372,393,429 | 322,417,477 | 505 | 595 | 17741 | 2.57 | 13863 | 0.60 |
| $BIQCH_3CH_3$ | 298,375,396,439 | 298,396,479 | 521 | 597 | 27797 | 2.53 | 14363 | 0.68 |
| $BIQCH_3Br$ | 300,311,376,439 | 332,424,488 | 515 | 596 | 17864 | 2.57 | 13915 | 0.61 |
| $BIQCH_3NO_2$ | 291,365,396,428 | 285,365,491 | 507 | 590 | 18155 | 2.58 | 14640 | 0.60 |

[a]Recorded in $10^{-5}$ mol $L^{-1}$ toluene and $10^{-3}$ mol $L^{-1}$ in thin solid film form.
[b]Extinction coefficient ( $L^{-1}mol^{-1}$ $cm^{-1}$) measured in toluene ($10^{-5}$ mol $L^{-1}$).
[c]Optical bandgap estimated from the optical edge of solution form. ( $\boldsymbol{E_g^{opt} = \frac{1240}{\lambda_{opt\ edge}}}$ )**eV**
[d]Stokes shift calculated from absorption and emission wavelength observed in solution form.
[e]Quantum yield with reference to $Alq_3$ ($\phi_F$ = 0.16 in benzene) [25].

$BIQCH_3$ and its derivatives **1–4** emits in green region with $\lambda_{em}$ at 505−521nm (**Fig. 2** (**a**)) upon excitation at their corresponding absorption maxima in toluene and in thin film form they emit in yellow region with $\lambda_{em}$ at 590−597 nm (**Fig. 2** (**b**)). The fluorescence spectra of $BIQCH_3$ and its derivatives **1–4** in thin solid film are nearly same order relative to solution form (**Fig. 2 (b)**). A significant bathochromic shift of 80 to 90 nm in thin solid film is observed. Red shift in thin film form of $BIQCH_3$ and its derivatives **1–4** is may be due to intermolecular aggregation of molecules in thin solid form.

Stokes shift ($\nu_{Abs} - \nu_{Em}$) indicates the difference in the structure and properties of the fluorescent molecule between ground and the excited states. The stokes shifts ($cm^{-1}$) were determined by Eq. (1),

$$(\nu_{Abs} - \nu_{Em}) = \left(\frac{1}{\lambda_{Abs}} - \frac{1}{\lambda_{Em}}\right) X\ 10^7 \quad (1)$$

The molecules show Stokes shifts with high values of 13863–14640 $cm^{-1}$ in toluene and are recorded at λmax value obtained from absorption spectra and fluorescence spectra, ensuring that there is no re-absorption of the emitted radiation.

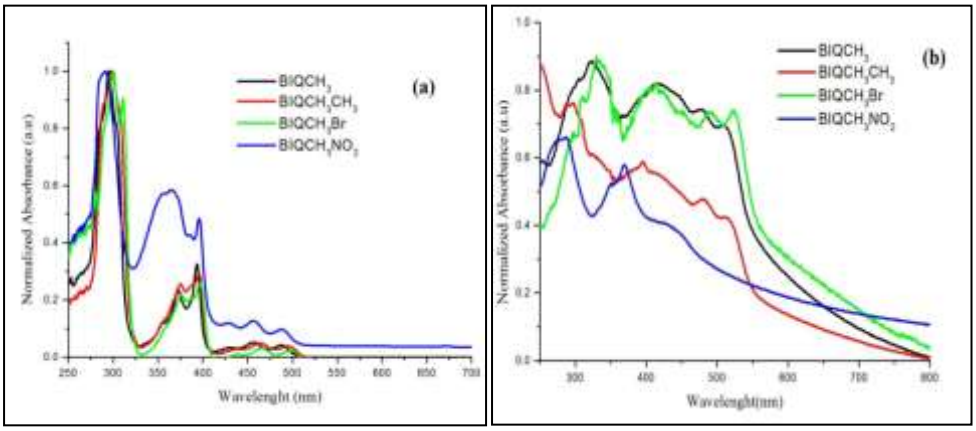


**Figure 1:** Normalized UV−Vis absorption spectra of $BIQCH_3$ and its derivatives **1–4** in toluene solution (**$10^{-5}$ mol $L^{-1}$**) (**a**) and in thin solid film form (**b**).

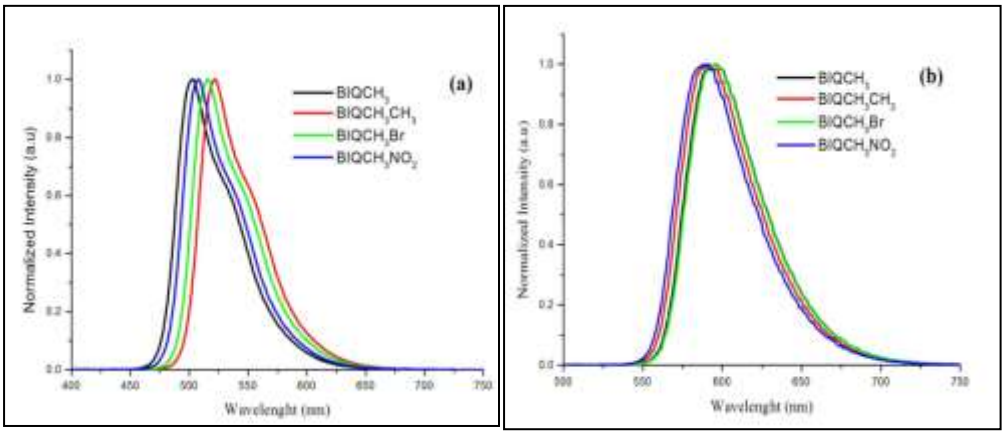


**Figure 2:** Normalized Fluorescence spectra of $BIQCH_3$ and its derivatives **1–4** in toluene solution (**$10^{-5}$ mol $L^{-1}$**) (**a**) and thin solid film form (**b**).

Fluorescence quantum yield is an important parameter for the characterization of optical materials to be used in OLEDs. The fluorescence quantum yield of the $BIQCH_3$ and its derivatives **1–4** were calculated using tris(8-hydroxyquinolinato)aluminium(III) ($Alq_3$) ($\phi_F$ = 0.16 in benzene) [25] as standard according to Eq. (2),

$$\text{Quantum efficiency } \phi_F = \phi_{ref}\left(\frac{S_{samp}}{S_{ref}}\right)\left(\frac{A_{ref}}{A_{samp}}\right)\left(\frac{\eta^2_{samp}}{\eta^2_{ref}}\right) \quad (2)$$

Where $S_{ref}$, $A_{ref}$, $\eta_{ref}$ and $S_{sample}$, $A_{sample}$, $\eta_{sample}$ represent the integrated emission band area, the absorbance at the excited wavelength, and the refractive index of the solvent, respectively for the standard reference and the sample. The quantum yields of the $BIQCH_3$ and its derivatives **1–4** are in the range 0.60–0.68 (**Table 1**).

The material performance for electroluminescence applications are evaluated by comparing the emission color by means of color coordinates. The CIE chromaticity coordinates of the $BIQCH_3$ and its derivatives **1–4** are determined using the emission spectra of the derivatives excited at 300 nm in thin film. The obtained CIE coordinates are located in the yellow green region. The CIE coordinates and chromaticity diagram are depicted in **Table 2** and **Figure 3** respectively.

Thus, the photophysical parameters indicate that the $BIQCH_3$ and its derivatives **1–4** are potential candidates for the fabrication of OLEDs.

**Table 2:** CIE coordinates of compounds **1–4**.

| Compound | CIE coordinates | |
|---|---|---|
| | x | y |
| $BIQCH_3$ | 0.444 | 0.418 |
| $BIQCH_3CH_3$ | 0.416 | 0.403 |
| $BIQCH_3Br$ | 0.465 | 0.419 |
| $BQCH_3NO_2$ | 0.438 | 0.426 |

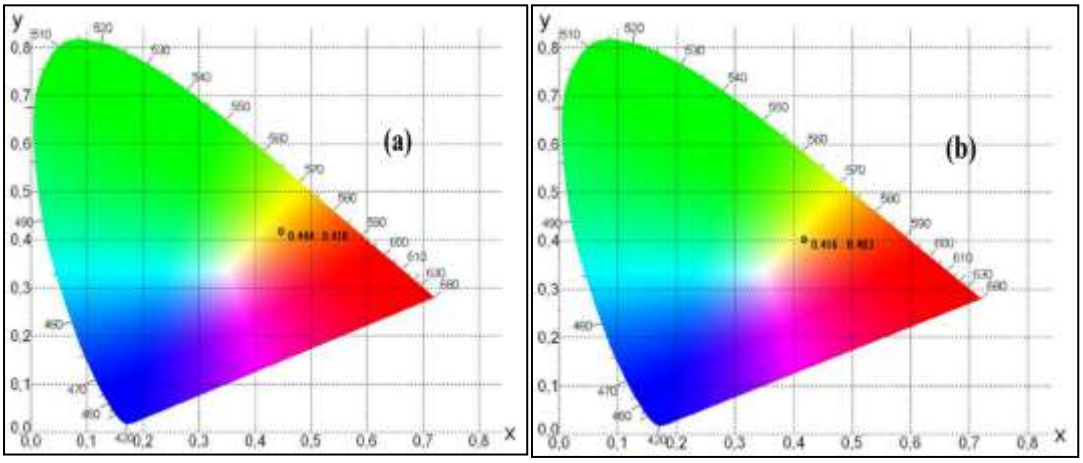


**Figure 3:** Chromaticity diagram of $BIQCH_3$ (**1**) (**a**) and $BIQCH_3CH_3$ (**2**) (**b**) in thin solid film. (For $BIQCH_3Br$ (**3**) and $BIQCH_3NO_2$ (**4**) see **supporting information**).

### 3.2 Electrochemical properties

Cyclic voltammetry was used to study the redox behavior of $BIQCH_3$ and its derivatives **1–4** and to determine their ionization potential (HOMO) and electron affinity (LUMO) energy levels. The HOMO

and LUMO energy levels of the materials are very crucial parameters for most of the electro optical devices, which guides the charge transport mechanics. The HOMO and LUMO of $BIQCH_3$ and its derivatives **1–4** lies in the range of 5.66−5.83 eV and 2.87−3.15 eV respectively. The observed parameters are reported in **Table 3**. The cyclic voltammogram are displayed in **Figure 4**.

**Table 3:** Electrochemical data of $BIQCH_3$ and its derivatives **1–4**.

| Compounds | $E_{ox}^{peak}$ [a] (V) | $E_{red}^{peak}$ [b] (V) | HOMO[c] (eV) | LUMO[d] (eV) | $E_g^{EC}$ [e] (eV) |
|---|---|---|---|---|---|
| **$BIQCH_3$** | 1.33 | −1.54 | −5.77 | −2.87 | 2.90 |
| **$BIQCH_3CH_3$** | 1.26,1.65 | −1.45, −1.85 | −5.66 | −2.96 | 2.70 |
| **$BIQCH_3Br$** | 1.33, 1.72 | −1.39, −1.81 | −5.73 | −3.02 | 2.71 |
| **$BIQCH_3NO_2$** | 1.43, 1.70 | −1.26, −1.45, −1.58, −1.89 | −5.83 | −3.15 | 2.68 |

[a] $E_{ox}^{peak}$ oxidation peak potential against $Fc/Fc^+$.

[b] $E_{red}^{peak}$ reduction peak potential against $Fc/Fc^+$.

[c] HOMO energy level calculated from $E_{HOMO} = -[E_{ox}^{peak} - E_{ox}(Fc/Fc^+) + 4.8]$ eV.

[d] LUMO energy calculated from $E_{LUMO} = -[E_{red}^{peak} - E_{red}(Fc/Fc^+) + 4.8]$ eV.

[e] $E_g^{EC}$ calculated from $E_g^{CV} =$ HOMO−LUMO.

On anodic sweep $BIQCH_3$ (**1**) show one irreversible peak and rest others show two irreversible peaks around 1.26−1.72 eV and which is may be due to oxidation of indole unit. On cathodic sweep $BIQCH_3$ (**1**) show one reversible peak and $BIQCH_3CH_3$ (**2**) and $BIQCH_3Br$ (**3**) shows two reversible peaks which may be correspond to formation of mono and diradical anion of quinoxaline unit [29]. $BIQCH_3NO_2$ (**4**) shows four irreversible reduction peak and peak at −1.26 eV is may be due to reduction of nitro group.

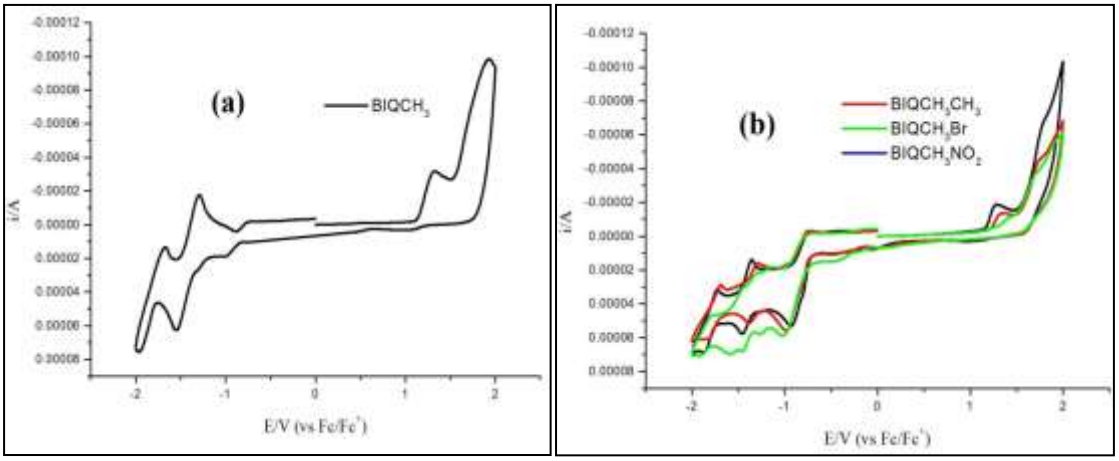


**Figure 4:** The cyclic voltammogram of $BIQCH_3$ (**1**) (**a**) and compounds **2–4** (**b**) ($10^{-3}$ **mol** $L^{-1}$) measured in dry $CH_2Cl_2$ solution against ferrocene/ferrocenium.

Increase in LUMO energy value is observed on substituting second position of $BIQCH_3$ (**1**) with electron withdrawing groups like –Br and $–NO_2$ (compounds **3** and **4**) is observed. This increase is in LUMO energy values of molecules $BIQCH_3Br$ (**3**) and $BIQCH_3NO_2$ (**4**) is due to increase in electron deficiency of electron rich indole unit and hence increases electron accepting property of quinoxaline unit. $BIQCH_3Br$ (**3**) and $BIQCH_3NO_2$ (**4**) may acts electron transporting material since their LUMO values are found above 3.0 eV [30]. The energy band gap determined from the cyclic voltammetry measurements are in range of 2.68–2.90 eV and are comparable with the optically calculated band gap.

**3. Thermal properties**

The electroluminescence devices containing π–conjugating organic materials should withstand temperature as high as 80 $^0$C [31,32]. The stability and lifetime of the device can be improved by possessing material with high thermal stability. The thermal stability of $BIQCH_3$ and its derivatives **1–4** was determined by Thermo gravimetric analysis (TGA) at the temperature range of 30–1000 $^0$C at a constant heating rate of 10 $^0$C $min^{-1}$ under nitrogen atmosphere. While the melting point of target molecules were less approximately determined by open capillary method. The observed TGA parameters for $BIQCH_3$ and its derivatives **1–4** are reported in **Table 4**. TGA thermograms and DTA Plots are displayed in **Figure 5**(**a**) and **Figure 6.** The derivative thermogram curves **Figure 5**(**b**) show two narrow derivative peaks indicating high decomposition temperature with $T_{max}$ in the range of 325–341$^0$C and 501–550 $^0$C respectively.

**Table 4:** Thermal data of $BIQCH_3$ and its derivatives **1–4**.

| Compounds | $T_m$ ($^0$C)[a] | $T_d$ ($^0$C)[b] | $T_{max}$($^0$C)[c] |
|---|---|---|---|
| $BIQCH_3$ | 238 | 260 (290) | 325, 521 |
| $BIQCH_3CH_3$ | 215 | 274 (300) | 341, 550 |
| $BIQCH_3Br$ | 274 | 248 (290) | 329, 501 |
| $BIQCH_3NO_2$ | >300 | 190 (220) | 336, 525 |

[a]Melting point (Open capillary Method)

[b]Decomposition temperature [5% and 10% (in parentheses) weight loss] derived by TGA.

[c]Derivative weight loss derived by TGA.

The DTA plot exhibit clear endothermic melting peak for all the prepared compounds except $BIQCH_3NO_2$ (**4**) and melting points obtained by open capillary method are in close agreement with DTA endothermic peaks.

TGA study reveals that the $BIQCH_3$ and its derivatives **1–4** exhibit good thermal stability and show two step thermal decomposition process. First step is may be due to loss of substituents at second position of indole unit and second step may be due to loss of entire Benz[*g*]indolo[2,3-*b*]quinoxaline backbone. The decomposition temperature corresponding to 5% and 10% weight loss were in the range of 190–274 $^0$C and 220–300 $^0$C respectively. The order of thermal stability among the $BIQCH_3$ and its

derivatives **1–4** is **4<3<1<2** (**Table 4**). Despite being relatively low molecular weight molecules, prepared compound show amorphous nature and high decomposition temperatures suggesting that they have high thermal stability and beneficial for the fabrication of amorphous thin film.

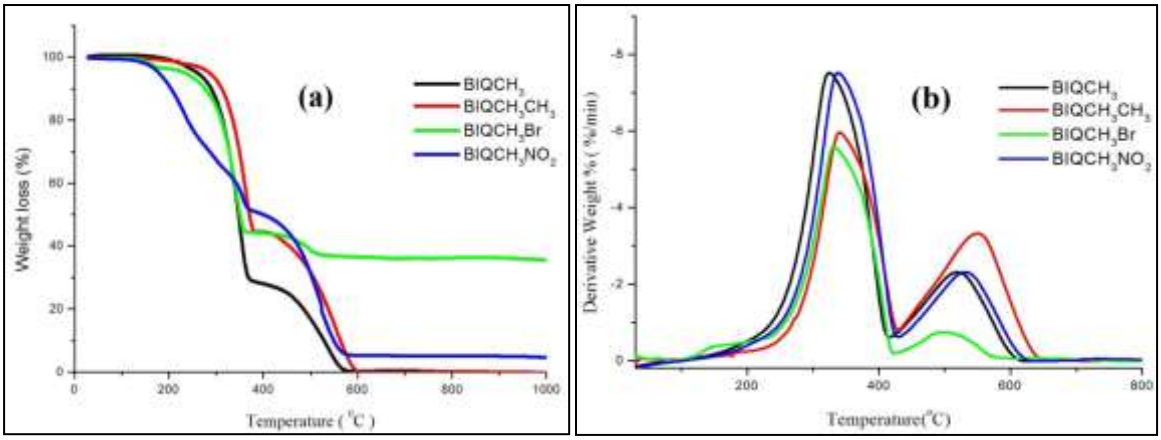


**Figure 5:** TGA thermogram (**a**) derivative weight loss (**b**) of $BIQCH_3$ and its derivatives **1–4** under nitrogen atmosphere at normal pressure, heating rate, $10^0$ C/$min^{-1}$.

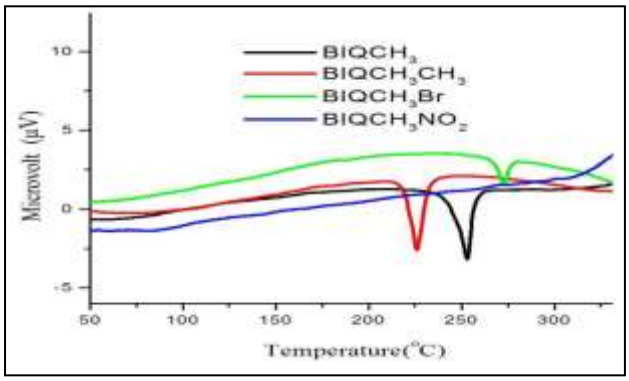


**Figure 6:** DTA thermogram of $BIQCH_3$ and its derivatives **1–4** under nitrogen atmosphere.

## 4. CONCLUSIONS

$BIQCH_3$ and its derivatives **1–4** have been prepared with good yield with optimum bandgap which is required for organic light emitting diodes (OLEDs) applications. The photophysical, electrochemical and thermal properties of the compounds are depend on Benz[*g*]indolo[2,3-*b*]quinoxaline core and substituents on its second position of indole unit. $BIQCH_3$ and its derivatives **1–4** emit in green and yellow color region in toluene and in solid state respectively. The electrochemical investigation of compounds show that the LUMO level increases on introduction of electron withdrawing group at second position of $BIQCH_3$. Further electrochemical bandgap are in close agreement with optical bandgap suggesting efficient charge separation and transportation. Thermal properties revealed that the derivatives have high melting point and good thermal stability. Thus above results indicate that the prepared molecules are promising candidate for OLED applications. Further, work is in progress in the direction of increasing LUMO energy value and decreasing bandgap by functionalization at second position of indole unit of Benz[*g*]indolo[2,3-*b*]quinoxaline core.

## ACKNOWLEDGEMENT

The authors are greatly thankful to Micro-Analytical Laboratory, Department of Chemistry, University of Mumbai for providing Instrumental facilities. One of the authors (Azam M. Shaikh) is grateful to University Grants Commission, India for providing fellowship.

## REFERENCES

[1] Tang, C. W.; VanSlyke, S. A. Organic electroluminescent diodes. *Appl. Phys. Lett.* **1987**, *51*, 913−915

[2] Friend, R. H.; Gymer, R. W.; Holmes, A. B.; Burroughes. J. H.; Marks. R. N.; Taliani. C.; Bradley. D. D. C.; dos Santos, D. A.; Bredas, J. L.; Logdlund. M.; Salaneck. W. R.; Electroluminescence in conjugated polymers. *Nature* **1999**, 397, 121–128.

[3] Baldo, M. A.; Thompson, M. E.; Forrest. S. R. High-efficiency fluorescent organic light-emitting devices using a phosphorescent sensitizer. *Nature* **2000**, 403, 750–753.

[4] Anthony, J. E. The larger acenes: versatile organic semiconductors. *Angew. Chem. Int. Ed.* **2008**, 47, 452−483.

[5] Imahori, H.; Umeyama, T.; Ito, S. Large π-aromatic molecules as potential sensitizers for highly efficient dye-sensitized solar cells. *Acc. Chem. Res*. **2009**, 42, 1809–1818.

[6] Ning, Z.; Tian, H. Triarylamine: a promising core unit for efficient photovoltaic materials. *Chem. Commun.* **2009**, 5483–5495.

[7] Gratzel, M. Recent advances in sensitized mesoscopic solar cells. *Acc. Chem. Res.* **2009**, 42, 1788−1798.

[8] Shirota, Y. J. Organic materials for electronic and optoelectronic devices Mater. *J. Mat. Chem*. **2000**, 01, 1−25.

[9] Pyszka, I.; Kucybala, Z.; Nikczynski, G. The dyes containing quinolines and quinoxalines skeleton as effective photoinitiator of free radicals polymerization. *Chemik* **2011**, 65(4), 283-290.

[10] Przyjazna, B.; Kucybała, Z.; Czkowski, J. P. Development of new dyeing photoinitiators based on 6H-indolo[2,3-b]quinoxaline skeleton. *Polymer* **2004**, 45, 2559–2566.

[11] Venkateswarao, A.; Tyagi, P.; Thomas, K. R. J.; Chen, P. W.; Ho, K. C. Organic dyes containing indolo[2,3–*b*]quinoxaline as a donor: Synthesis, Optical and photovoltaic properties. *Tetrahedron* **2014**, 70, 6318–6327.

[12] Su, T-H.; Fan, C-H.; Yang, Y-H.; Hsu, L-C.; Chemg, C-H. Highly efficient deep-red organic electrophosphorescent devices with excellent operational stability using bis(indoloquinoxalinyl) derivatives as the host materials. *J. Mater. Chem. C*. **2013,** 1, 5084–5092.

[13] Tyagi, P.; Venkateswararao, A.; Thomas, K. R. J. Pyrene-based organic dyes with thiophene containing p-linkers for dye-sensitized solar cells *J. Org. Chem.* **2011**, **76**, 4571–4581.

[14] Thomas, K. R. J.; Tyagi, P. Synthesis, Spectra, and Theoretical Investigations of the Triarylamines based on 6H-Indolo[2,3-b]quinoxaline. *J. Org. Chem*. **2010**, 75, 8100–8111.

[15] Harmenberg, J.; Bergman, W. J. A. N.; Akerfeldt, S.; Lundlad, L. Antiherpesvirus activity and mechanism of action of indolo[2,3-b]quinoxaline and analogs. *Antimicrob.Agents Chemother*. **1988**, 32, 1720–1724.

[16] Harmenberg, A.; Malmfors, G.T.; Bergman, J.; Wahren, B.; Cox, S. The mechanism of action of the anti-herpes virus compounds 2,3-dimethyl-6(2-dimethyl)-6*H*-indolo-[2,3,-*b*]quinoxaline. *Antiviral Res*. **1991**, 15, 193–204

[17] Hirata, J.; Araya, S.; Nakaike, K. K.; Ishida, T. Side chain-dependent of antitumor indoloquinoxaline derivatives to DNA: comparative spectroscopic and viscometric measurement. *Chem. Pharm. Bull.* **2001**, 49, 44–48.

[18] Deady, L.W.; Kaye, A.J.; Finlay, G.J.; Baguley, B.C.; Denny, W.A. Synthesis and antitumor properties of N-[2-(dimethylamino)ethyl]carboxamide derivatives: a new class of putative topoisomerase inhibitors. *J. Med. Chem*. **1997**, 40, 2040–2046.

[19] Manna, K.; Agrawal, Y. K. Microwave assisted synthesis of new indophenazine 1,3,5, tri substituted pyrazoline derivatives of benzofuran and their antimicrobial activity. *Bioorg. Med. Chem. Lett.* **2009**, 19, 2688–92.

[20] Pai, N. R.; Pusalkar, D. A. Pharmacological screening of novel indolo[2,3-b]quinoxaline derivatives. *J. Chem. Pharm. Res.* **2010**, 2, 485–493.

[21] Drushlyak, A. G.; Ivashchenko, A. V.; Titov, V. V. Reaction of aromatic o-diamines with isatin with 2,3−diaminonaphthalene. *Khim. Getero. Soed*. **1984**, 10, 1399−1403

[22] Popp.; Frank, D. Reaction of isatin with aromatic o−diamines. *J. Hetero .Chem.* **1969**, 6(1), 125−127.

[23] Smith, C. D.; Myers, C. B.; Zilfou, J. T.; Smith, S. N.; Lawrence, D. S. Indoloquinoxaline compounds that selectively antagonize P-glycoprotein. *Oncology Research* **2001**, 12(5), 219−229.

[24] Loregian, A.; Coen, D. M. Selective Anti-Cytomegalovirus compound discovered by screening for inhibitor of subunit interaction of the viral polymerase. *Chemistry & Biology* **2006**, 13(2), 191−200.

[25] Katsuta, S. Fluorescence enhancement of aluminum (III) 8-quinolinolate in the presence of 3,5-Dichlorophenol. *Chem. Lett*. **1994**, 1239–1242.

[26] Tarek, A. F.; Fayzah, A. S. B. J; Omima, A. W. Schiff bases of indoline-2,3-dione(isatin) derivatives and nalidixic acid carbohydrazide, synthesis, antitubercular activity and pharma cophoric model building. *Eur. J. Med. Chem.* **2010,** 45 4578–4586.

[27] Beauchard.; Ferandin, A.; Yoan, F.; Lozach, S.; Blairvacq, O.; Meijer, M.; Thiery, L.; Besson, V.; Thierry. Synthesis of novel 5-subsituted indirubin as protein kinases inhibitor. *Bioorg. Med. Chemistry*. **2006**, 14(18), 6434–6443.

[28] Rajini, P.; Aruna, D.; Raghunandan, N.; Venkateshwar, R. J. Synthesis and screening of new isatin derivatives. *J. Pharm. Res*. **2013**, 2(11), 3–5.

[29] Armand, J.; Boulares, L.; Bellec, C.; Pinson, J.; .Electrochemical reduction of quinoxalino[2,3-*b*]quinoxaline. *Can. J. Chem*. **1982**, 60, 2797–2803.

[30] Newmann, C. R.; Frisbie, C. D.; da Silva Filho D. A.; Bredas, J.; Ewbank, P. C.; Mann, K. R. Introduction to organic thin film transistor and design of n-channel organic semiconductor. *Chem .Mater*. **2004**, 16, 4436–4451.

[31] Hamal, S.; Hirayama, F. Actinometric Determination of Absolute Fluorescence Quantum Yields. *J. Phys. Chem*. **1983**, 87, 83–88.

[32] Osaheni, J. A.; Jenekhe, S. A. Efficient blue luminescence of a conjugated polymer exciplex. *Macromolecules* **1994**, 27, 739–742.

*The authors declare no conflict of interest*

© 2015 By the Authors; Licensee Borderless Science Publishing, Canada. This is an open access article distributed under the terms and conditions of the Creative Commons Attribution license http://creativecommons.org/licenses/by/3.0